

Updated sensitivities to heavy neutral leptons at the LHC far detectors and SHiP

Zeren Simon Wang^{1,*} and Yu Zhang^{1,†}

¹*School of Physics, Hefei University of Technology, Hefei 230601, People's Republic of China*

In recent years, a number of experiments dedicated to searches for long-lived particles (LLPs) have been proposed, approved, or have entered operation. While the sensitivities of these experiments to various LLP scenarios have been extensively studied, key aspects—such as detector geometries, background estimates, and projected operational durations—for several facilities, including MATHUSLA, ANUBIS, and SHiP, have undergone significant updates. In this work, we implement the latest experimental designs in the Displaced Decay Counter tool for calculating detector acceptances and signal-event yields, and re-evaluate their sensitivity reach to one of the most widely studied LLP scenarios, namely minimal heavy neutral leptons.

Introduction. The Large Hadron Collider (LHC) at CERN culminated in the discovery of a Standard-Model (SM)-like Higgs boson in 2012 [1, 2]. Continuing searches for physics beyond the SM (BSM) have so far yielded no positive signals, while increasingly stringent lower bounds have been placed on the masses of heavy fundamental particles predicted in various BSM scenarios, such as supersymmetry (SUSY); see Refs. [3, 4] for reviews, and also Refs. [5–7] for recent summaries of the current status and future prospects of SUSY searches at the LHC and high-luminosity LHC (HL-LHC). In particular, current lower bounds on superpartner masses at the TeV scale imply a large degree of fine-tuning, rendering supersymmetry no longer a natural solution to the hierarchy problem of the SM [8].

This situation has led both theorists and experimentalist to re-examine existing search strategies for BSM physics. One possibility is that new physics does not manifest itself through heavy states that decay promptly after production, but instead through long-lived particles (LLPs). LLPs are predicted to give rise to a rich variety of exotic and unconventional signatures at terrestrial experiments, including colliders and beam-dump facilities; see Refs. [9–14] for reviews on both theoretical and experimental perspectives.

The LHC collaborations have undertaken extensive efforts to search for LLPs; see Refs. [15–20] for a selection of recent results reported by ATLAS, CMS, and LHCb. Although no LLP predicted in BSM scenarios has been discovered to date, increasingly strong exclusion limits have been obtained. In addition to the LHC main detectors, several dedicated experiments for LLP searches have been proposed, approved, or have already begun operation. In these experiments, LLPs produced at the interaction point (IP) are expected to travel macroscopic distances before potentially decaying inside dedicated fiducial volumes. Such experiments include a class of far detectors installed at distances of roughly 10–600 m from different LHC IPs, as well as a beam-dump experiment, the Search for Hidden Particles (SHiP) [21–27].

Among the proposed LHC far-detector experiments, FASER [28–30] has been operating since 2022 and has already published its first results [31, 32]. Other proposals include ANUBIS [33, 34], CODEX-b [35, 36], FACET [37], FASER2 [38], MoEDAL-MAPP1 and MAPP2 [39, 40], and MATHUSLA [11, 41–44]. The SHiP experiment has been approved in 2024 and is currently planned to begin commissioning and first data-taking between 2031 and 2033 [27, 45]. Sensitivity projections for these experiments across a wide range of LLP scenarios have been extensively studied; see e.g., Refs. [46–51] for recent phenomenological works.

Very recently, the overall plans of several of these experiments have undergone major revisions, most notably for MATHUSLA [44] and ANUBIS [34]. The planned fiducial volume of MATHUSLA has been substantially reduced, and the proposed location of the ANUBIS detector has been changed from a service shaft to the cavern hosting the ATLAS detector, with the ANUBIS detector installed on the cavern ceiling. The SHiP experiment employs its Hidden Sector Decay Spectrometer (HSDS) as the decay volume for LLPs, and while its geometry has also been updated, the changes are comparatively modest. In addition, its projected operational duration has been updated to 15 years, which we adopt in this work.

For most of the experiments considered here, the large distances from the IPs allow for the installation of shielding and veto systems, leading to expectations of negligible background levels. An important exception is ANUBIS, for which the revised detector design implies significantly different background conditions. These have been carefully evaluated in Ref. [34].¹ The updated background levels have a substantial impact on the sensitivity reach and are therefore taken into account in our numerical analysis.

Taken together, these recent developments motivate a timely re-assessment of the sensitivity projections for LLP searches at the LHC far detectors and SHiP, as well as a re-evaluation of their relative performance.

A wide variety of BSM scenarios predict LLPs. In this

* wzs@hfut.edu.cn

† dayu@hfut.edu.cn

¹ A complementary discussion of background estimates at ANUBIS can be found in Appendix B of Ref. [46].

work, we focus on heavy neutral leptons (HNLs) [52–54], also commonly referred to right-handed neutrinos, heavy neutrinos, or sterile neutrinos.² HNLs are SM-singlet fermions that mix with active neutrinos. While HNLs can also appear in non-minimal scenarios involving additional BSM degrees of freedom [56–59], here we focus on the minimal scenario in which HNLs constitute the only new states. This provides a clean benchmark for comparing detector sensitivities without introducing additional model-dependent parameters. Although many models predict three generations of HNLs, we assume for simplicity that only a single HNL, denoted by N , is kinematically accessible, with the remaining states sufficiently heavy to decouple. We further assume that N mixes exclusively with the electron neutrino. This benchmark scenario has been widely adopted in studies of the experimental sensitivity to HNLs. Finally, we restrict our attention to HNLs produced in decays of heavy mesons. For existing studies on the sensitivity reach of the LHC far detectors and SHiP to the minimal HNLs, see, e.g., Refs. [11, 23, 29, 60–67]; see also early proposals to search for HNLs at accelerator-based experiments in e.g. Refs. [68, 69].

In this work, we implement the latest designs of the experiments discussed above in the public tool Displaced Decay Counter (DDC) [70, 71] to compute the acceptances of the LHC far detectors and SHiP for long-lived HNLs. Based on these acceptances, we evaluate the corresponding sensitivity reach, shown in Fig. 1. These updated results show, as expected, important changes in the sensitivity projections for MATHUSLA and ANUBIS particularly, comparing their latest designs with their previous configurations. Details of the experimental configurations and the simulation procedure underlying these results are described in the following sections. These results provide a useful reference for comparing the constraining power of the considered experiments for LLPs produced in heavy-meson decays at the LHC and at SHiP.

Model. After spontaneous electroweak symmetry breaking, the relevant interactions of the heavy neutral lepton are described by the Lagrangian

$$\mathcal{L}_N = \frac{g}{\sqrt{2}} \sum_{\alpha} V_{\alpha N} \bar{\ell}_{\alpha} \gamma^{\mu} P_L N W_{L\mu}^{-} + \frac{g}{2 \cos \theta_W} \sum_{\alpha, i} V_{\alpha i}^L V_{\alpha N}^* \bar{N} \gamma^{\mu} P_L \nu_i Z_{\mu}, \quad (1)$$

where g denotes the SU(2) gauge coupling, $V_{\alpha N}$ parameterizes the mixing between the active neutrino ν_{α} and the HNL N with $\alpha = e, \mu, \tau$, V^L is the left-handed neutrino mixing matrix, and θ_W is the Weinberg angle.

We assume the HNL to be a Majorana fermion. HNLs can be produced in rare, prompt, leptonic and semi-

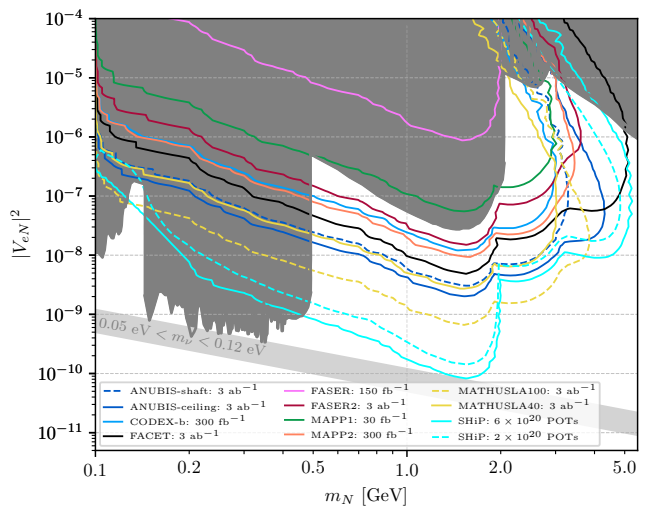


FIG. 1. Updated sensitivity reach of the LHC far detectors and the SHiP beam-dump experiment to minimal heavy neutral leptons that mix with the electron neutrino only, shown in the $(m_N, |V_{eN}|^2)$ plane. The dark gray area represents the current experimental bounds obtained at PIENU [72], KENU [73], CHARM [74], NA62 [75, 76], T2K [77], BEBC [78], DELPHI [79], ATLAS [80], and CMS [81]. The light gray band corresponds to the parameter region targeted by the type-I seesaw mechanism for active-neutrino masses between 0.05 eV and 0.12 eV. The sensitivity in the low-mass region ($m_N \lesssim m_D$) is dominated by HNLs produced from charm-meson decays, whereas for heavier masses ($m_D \lesssim m_N \lesssim m_B$) the contribution from bottom-meson decays dominates; only D - and B -meson channels are included in this analysis. The sensitivities of the outdated designs are displayed as dashed lines.

leptonic decays of charm and bottom mesons,³ and subsequently decay via both charged-current and neutral-current interactions into lighter SM particles. Throughout this work, we follow Ref. [65] for the calculation of meson decay branching ratios (BRs) into HNLs, as well as for the computation of HNL decay widths. We will study the range of HNL masses between 0.1 GeV and the B -meson thresholds.

Experiments & simulation. As discussed in the first section, we study LHC far-detector experiments and the SHiP beam-dump experiment. We will first elaborate on the experiments of which the geometrical designs have been significantly changed and hence for which the discovery prospects of LLPs should be largely modified. These experiments are MATHUSLA and ANUBIS.

MATHUSLA was initially proposed as a rectangular box with the dimensions of 200 m \times 200 m \times 20 m for its fiducial volume, to be 100 m distanced both vertically (y -axis) and horizontally (z -axis) from the ATLAS or CMS IP [11, 41, 42]. In its updated Letter of Intent [43], the

² See Ref. [55] for a recent overview of the present and future status of the HNLs.

³ We neglect HNL production from pion, kaons, and heavier mesons in this work.

geometrical design has changed to $100\text{ m} \times 100\text{ m} \times 25\text{ m}$, positions with a horizontal (vertical) distance of 68 m (60 m) from the CMS IP; we coin this configuration as MATHUSLA100. In the lately published Conceptual Design Report for MATHUSLA [44], for cost reasons the fiducial volume has further shrunk, now to $40\text{ m} \times 40\text{ m} \times 11\text{ m}$ (MATHUSLA40). It is supposed to be 70 m and 81 m away from the CMS IP in the z - and y -directions, respectively.

The geometrical configuration of ANUBIS has been critically updated, too. Originally proposed to be installed inside one of the service shafts above the ATLAS IP, ANUBIS-shaft [33]⁴ should be 5 m and 24 m away from the ATLAS IP in z - and y -directions. It is cylindrically shaped with a height of 56 m and a diameter of 18 m. The LLPs are supposed to decay inside this cylinder with the charged decay products to hit on three track stations inside. The latest design of ANUBIS [34] takes a distinct direction, now exploiting the space between the ATLAS main detector and the cavern ceiling as the fiducial volume. It has a shape of an annular cylindrical sector of length 53 m; its inner and outer radii are 11.3 m and 19.3 m; and it has an azimuthal coverage of $\sim 20\%$. Compared to ANUBIS-shaft, ANUBIS-ceiling is closer to the IP, guaranteeing both better acceptance rates and exacerbated background levels.

Besides MATHUSLA and ANUBIS, SHiP has its designs updated, though not to a large degree. We only list the geometrical dimensions of the latest design here, extracted from Ref. [25].⁵ The near end of the SHiP-HSDS which is the decay volume for the LLPs at the SHiP experiment, is 33 m away behind the target. The HSDS has a length of 50 m, and its front (rear) face has dimensions $(x, y) = 1.0\text{ m} \times 2.7\text{ m}$ ($4.0\text{ m} \times 6.0\text{ m}$). It is worth mentioning that compared to the relatively mild updates in its geometries, the SHiP experiment has its primary update in its projected operation period, now prolonged from 5 years to 15 years.

We also refer to the tool SensCalc [82] which, similarly, includes the implementations of ANUBIS-shaft, ANUBIS-ceiling, and the latest configuration of SHiP. The geometrical setups of these experiments in DDC, as we have checked, are in agreement with those in SensCalc.

For summaries of the other proposals considered in this work, we refer to e.g., Refs. [49, 65, 67]. They have all been implemented in DDC and in this work we rely on DDC to derive their sensitivity reach.

As mentioned above, we will focus on HNLs produced from rare decays of charm and bottom mesons. Concretely, we will consider the $D^0, D^+, D_s^+, B^0, B^+, B_s$ mesons, as well as their charge-conjugated counterparts. The production rates of these mesons, estimated for a 4π

solid-angle coverage [65, 83], are reproduced here:

$$\begin{aligned} N_{D^0+\bar{D}^0}^{\text{HL-LHC}} &= 3.89 \times 10^{16}, N_{D^++D^-}^{\text{HL-LHC}} = 2.04 \times 10^{16}, \\ N_{D_s^++D_s^-}^{\text{HL-LHC}} &= 6.62 \times 10^{15}, N_{D^0+\bar{D}^0}^{\text{SHiP}} = 1.29 \times 10^{18}, \\ N_{D^++D^-}^{\text{SHiP}} &= 4.2 \times 10^{17}, N_{D_s^++D_s^-}^{\text{SHiP}} = 1.8 \times 10^{17}, \\ N_{B^0+\bar{B}^0}^{\text{HL-LHC}} &= 1.46 \times 10^{15}, N_{B^++B^-}^{\text{HL-LHC}} = 1.46 \times 10^{15}, \\ N_{B_s^0+\bar{B}_s^0}^{\text{HL-LHC}} &= 2.53 \times 10^{14}, N_{B^0+\bar{B}^0}^{\text{SHiP}} = 8.1 \times 10^{13}, \\ N_{B^++B^-}^{\text{SHiP}} &= 8.1 \times 10^{13}, N_{B_s^0+\bar{B}_s^0}^{\text{SHiP}} = 2.16 \times 10^{13}, \end{aligned} \quad (2)$$

where we assume an integrated luminosity of 3 ab^{-1} for the HL-LHC and a nominal 15-year operation of SHiP corresponding to 6×10^{20} protons on target (POTs).⁶

We then implement the latest geometries of MATHUSLA40, ANUBIS-ceiling, as well as SHiP-HSDS into the tool DDC which is then ready for calculating the acceptances of all the LHC far detectors and SHiP to the minimal HNLs. We proceed by computing the signal-event rates with the following expressions,

$$N_S^{N,D} = \sum_{M_D} N_{M_D} \cdot \mathcal{B}(M_D \rightarrow N + X) \cdot \epsilon_D \cdot \mathcal{B}(N \rightarrow \text{vis.}), \quad (3)$$

$$N_S^{N,B} = \sum_{M_B} N_{M_B} \cdot \mathcal{B}(M_B \rightarrow N + X) \cdot \epsilon_B \cdot \mathcal{B}(N \rightarrow \text{vis.}), \quad (4)$$

where we have split the computation into two parts, for D -meson and B -meson decays, respectively, and assumed that the kinematics of the HNLs produced from different charm mesons are approximately identical (the same for the different bottom mesons). The number of D - and B -mesons N_{M_D} and N_{M_B} are given in Eq. (2), and $\mathcal{B}(N \rightarrow \text{vis.})$ is the decay branching ratio of the HNL into visible final states for which we assume all the decay channels of N except the fully invisible tri-neutrino one are detectable. Finally, ϵ_D and ϵ_B are estimated with DDC.

DDC loads Pythia8 [84] for simulating hard QCD $c\bar{c}$ and $b\bar{b}$ events. Pythia8 performs showering and hadronization, and the simulated D - and B -mesons are set to decay exclusively into the HNL with the relative branching ratios between the different channels aligned with the meson-decay BR computation results. DDC then takes into account the kinematics of the HNLs provided by Pythia8, the geometries and positions of the considered detectors, as well as the HNL masses, and makes use of exponential decay distribution formula to calculate the acceptances:

$$\epsilon_{D/B} = \frac{1}{N_{\text{MC}}} \sum_{i=1}^{N_{\text{MC}}} \epsilon_i, \quad (5)$$

$$\epsilon_i = \frac{\delta\phi}{2\pi} e^{\left(-\frac{D}{\beta_i \gamma_i c\tau_N}\right)} \left(1 - e^{-\frac{L}{\beta_i \gamma_i c\tau_N}}\right), \quad (6)$$

⁴ See also Ref. [64] for one of the first LLP sensitivity studies of ANUBIS-shaft.

⁵ We refer to Refs. [26, 65] for detail of the previous geometrical design of SHiP, which is not largely different from the latest design.

⁶ In the previous design of the SHiP experiment [26], a period of 5 years corresponding to 2×10^{20} POTs was planned.

where N_{MC} is the total number of Monte-Carlo simulation events (we have simulated ten thousand or one hundred thousand events for each mass point in different cases), $\delta\phi$ is the azimuthal-angle coverage of the detector, D is the distance between the hard-collision point and the detector along the traveling direction of the HNL, L is the distance that the HNL would travel inside the detector if it does not decay before leaving the detector, β_i and γ_i are the speed and Lorentz boost factor of the i^{th} simulated HNL, c labels the speed of light, and τ_N is the HNL's mean lifetime. We assume 100% detection efficiency for the visible decays. For more detail of the computation procedure applied in DDC for the different detectors, see Ref. [70].

As discussed earlier, we would assume zero background for all the experiments except **ANUBIS-shaft** and **ANUBIS-ceiling**. The background levels of LLP searches at **ANUBIS-ceiling** and **ANUBIS-shaft** have been estimated in Ref. [34], which reports 182.4 ± 12.2 and 63.7 ± 4.3 , respectively. Following Ref. [64] we take $N_{S95}^{\text{ANUBIS-ceiling}} = 2 \times \sqrt{195} \approx 28$ and $N_{S95}^{\text{ANUBIS-shaft}} = 2 \times \sqrt{68} \approx 17$ as the signal-event numbers corresponding to the exclusion limits at 95% confidence level (C.L.) for the two **ANUBIS** configurations, respectively. For the zero-background experiments, we show contour curves for 3 signal events as the sensitivity reach at 95% C.L.

Results. The numerical results are displayed in Fig. 1 in the $(m_N, |V_{eN}|^2)$ plane where the contour curves are exclusion boundaries at 95% C.L. For each experiment, the sensitivities are dominated by the charm-meson (bottom-meson) contributions for $m_N \lesssim m_D$ ($m_D \lesssim m_N \lesssim m_B$), mainly as a result of the charm-meson productions rates several orders of magnitude larger than those of the bottom mesons. The sensitivity reaches of the up-to-date designs are shown with solid lines, while those of the outdated ones with dashed curves. We find that for $m_N \lesssim m_D$ the sensitivity reach is dominated by **SHiP**, followed by **MATHUSLA100** and **ANUBIS-ceiling**, while for heavier HNLs **MATHUSLA100** and again **SHiP** are expected to dominate the sensitivity reach. We note that the sensitivity results of the non-updated LLP experiments (such as **FASER** and **CODEX-b**) that we obtained with DDC are, as we checked, in excellent agreement with those reported in the existing literature [11, 23, 29, 60–67].

The dark-gray regions have been excluded, representing a combination of the constraints obtained at **PIENU** [72], **KENU** [73], **CHARM** [74], **NA62** [75, 76], **T2K** [77], **BEBC** [78], **DELPHI** [79], **ATLAS** [80], and **CMS** [81]. Also, we present a band in light gray, corresponding to the parameter region targeted by the type-I seesaw relation, $|V_{eN}|^2 \simeq m_\nu/m_N$, for active-neutrino masses between 0.05 eV and 0.12 eV; the two values of the active-neutrino masses are inspired by neutrino-oscillations observations [85] and cosmological observations [86], respectively. In general we find almost all of the considered experiments can probe large parameter regions beyond the present bounds. **FASER** cannot test any unex-

cluded parameter region mainly because of its relatively small volume and limited dataset it is expected to receive (150 fb^{-1}).

As expected from considerations of detector volumes, **MATHUSLA40** is found to only probe $|V_{eN}|^2$ values larger than **MATHUSLA100** can by a factor of about 5. Meanwhile, its exclusion limits turn out to agree well with those of **ANUBIS-shaft** except when $m_N \gtrsim 2.8 \text{ GeV}$ where **ANUBIS-shaft** performs better mainly because it is more transverse. **ANUBIS-ceiling** is closer to the **ATLAS IP** than **ANUBIS-shaft**, thus resulting in both higher background levels and enhanced acceptances. Our numerical simulations show that **ANUBIS-ceiling** can test the mixing parameter squared smaller than **ANUBIS-shaft** can by approximately 2. Also, the latest design of the **SHiP** experiment is found to outperform the previous one by roughly a factor of 2 in testing $|V_{eN}|^2$, which is dominantly the consequence of the enhanced POT rates.

We note that while we have confined ourselves to considering an HNL mixed with the electron neutrino only, sensitivities for an HNL mixed with the muon neutrino only would be quite similar except for some minor effects of kinematic thresholds. As for an HNL mixed solely with the tau neutrino, tangibly reduced sensitivity reach is expected, because of relatively stronger suppression effects of kinematic thresholds and worse reconstruction efficiencies of the τ -leptons.

In addition, in the present paper we have assumed a Majorana HNL; if the HNL is of Dirac nature, the decay widths of the HNL should be reduced by a factor of 2 and the lower sensitivity reach of the studied experiments is correspondingly weakened by $\sim \sqrt{2}$.

Summary. In this work, we have implemented the updated geometrical designs of **MATHUSLA**, **ANUBIS**, and **SHiP** in the public tool DDC to compute the signal acceptances and event yields for a long-lived heavy neutral lepton mixed with the electron neutrino only. In particular, we incorporate the recently updated background estimates for **ANUBIS** reported in Ref. [34], going beyond the commonly adopted optimistic assumption of vanishing background, and account for the latest projected operational duration of the **SHiP** beam-dump experiment of 15 years.

Compared to **MATHUSLA100**, the reduced fiducial volume of **MATHUSLA40** leads to a sensitivity to the mixing parameter squared $|V_{eN}|^2$ weakened by a factor of ~ 5 , rendering it broadly competitive with the **ANUBIS-shaft** configuration except in the high-mass regime. The **ANUBIS-ceiling** setup, benefiting from its closer proximity to the IP, is expected to probe values of $|V_{eN}|^2$ smaller than those accessible to **ANUBIS-shaft** by a factor of ~ 2 . The latest plan of **SHiP** can exclude $|V_{eN}|^2$ values smaller than those the previous plan can by a factor of about 2, primarily owing to the relatively modest changes in its geometries and the currently 3-times prolonged operation period. The **SHiP** experiment, with its latest design, is found to dominate the sensitivity reach for m_N

just below the charm threshold and in the mass window $3.8 \text{ GeV} \lesssim m_N \lesssim 5.2 \text{ GeV}$, while MATHUSLA100 provides the strongest reach in the intermediate mass range.

With this short paper, we provide the LLP community with a concise, up-to-date reference on the sensitivity reach of the LHC far detectors and SHiP to one of the most widely studied LLP scenarios, namely minimal heavy neutral leptons. While our study focuses on minimal HNLs, the same procedure can readily be applied to non-minimal HNL scenarios or other LLP models, al-

lowing rapid assessment of the updated detector designs studied here for a broader class of BSM signatures.

Acknowledgments. Z.S.W. would like to thank Martin Hirsch for introducing him to the study of long-lived particles, including heavy neutral leptons, and for eight years of close collaboration. This work was supported by the National Natural Science Foundation of China under grant Nos. 12475106 and 12505120, and the Fundamental Research Funds for the Central Universities under Grant No. JZ2025HGTG0252.

-
- [1] G. Aad *et al.* (ATLAS), Phys. Lett. B **716**, 1 (2012), arXiv:1207.7214 [hep-ex].
- [2] S. Chatrchyan *et al.* (CMS), Phys. Lett. B **716**, 30 (2012), arXiv:1207.7235 [hep-ex].
- [3] H. P. Nilles, Phys. Rept. **110**, 1 (1984).
- [4] S. P. Martin, Adv. Ser. Direct. High Energy Phys. **18**, 1 (1998), arXiv:hep-ph/9709356.
- [5] H. Kwon (ATLAS, CMS) (2025) arXiv:2506.06839 [hep-ex].
- [6] J. Sonneveld (ATLAS, CMS) (2025) arXiv:2507.16400 [hep-ex].
- [7] H. Baer, V. Barger, J. Bolich, J. Dutta, D. Martinez, S. Salam, D. Sengupta, and K. Zhang, Rev. Mod. Phys. **97**, 045001 (2025), arXiv:2502.10879 [hep-ph].
- [8] G. F. Giudice, “The Dawn of the Post-Naturalness Era,” in *From My Vast Repertoire ...: Guido Altarelli’s Legacy*, edited by A. Levy, S. Forte, and G. Ridolfi (2019) pp. 267–292, arXiv:1710.07663 [physics.hist-ph].
- [9] J. Alimena *et al.*, J. Phys. G **47**, 090501 (2020), arXiv:1903.04497 [hep-ex].
- [10] L. Lee, C. Ohm, A. Soffer, and T.-T. Yu, Prog. Part. Nucl. Phys. **106**, 210 (2019), [Erratum: Prog.Part.Nucl.Phys. 122, 103912 (2022)], arXiv:1810.12602 [hep-ph].
- [11] D. Curtin *et al.*, Rept. Prog. Phys. **82**, 116201 (2019), arXiv:1806.07396 [hep-ph].
- [12] J. Beacham *et al.*, J. Phys. G **47**, 010501 (2020), arXiv:1901.09966 [hep-ex].
- [13] L. Jeanty and B. Shuve, (2025), arXiv:2511.17934 [hep-ph].
- [14] J. Alimena *et al.*, in *LHCb FIP Physics Workshop 2025* (2025) arXiv:2510.05257 [hep-ph].
- [15] G. Aad *et al.* (ATLAS), (2025), arXiv:2510.12347 [hep-ex].
- [16] G. Aad *et al.* (ATLAS), Phys. Rev. D **112**, 092001 (2025), arXiv:2503.20445 [hep-ex].
- [17] V. Chekhovsky *et al.* (CMS), JHEP **08**, 156 (2025), arXiv:2503.16699 [hep-ex].
- [18] A. Hayrapetyan *et al.* (CMS), (2025), arXiv:2511.08212 [hep-ex].
- [19] R. Aaij *et al.* (LHCb), Eur. Phys. J. C **82**, 373 (2022), arXiv:2110.07293 [hep-ex].
- [20] R. Aaij *et al.* (LHCb), (2025), arXiv:2512.14551 [hep-ex].
- [21] M. Anelli *et al.* (SHiP), (2015), arXiv:1504.04956 [physics.ins-det].
- [22] S. Alekhin *et al.*, Rept. Prog. Phys. **79**, 124201 (2016), arXiv:1504.04855 [hep-ph].
- [23] C. Ahdida *et al.* (SHiP), JHEP **04**, 077 (2019), arXiv:1811.00930 [hep-ph].
- [24] C. Ahdida *et al.* (SHiP), Eur. Phys. J. C **82**, 486 (2022), arXiv:2112.01487 [physics.ins-det].
- [25] R. Albanese *et al.* (SHiP), *BDF/SHiP at the ECN3 high-intensity beam facility*, Tech. Rep. (CERN, Geneva, 2023, CERN-SPSC-2023-033, SPSC-P-369).
- [26] C. Ahdida *et al.* (SHiP), JINST **14**, P03025 (2019), arXiv:1810.06880 [physics.ins-det].
- [27] R. Albanese *et al.* (SHiP, HI-ECN3 Project Team), (2025), arXiv:2504.06692 [hep-ex].
- [28] J. L. Feng, I. Galon, F. Kling, and S. Trojanowski, Phys. Rev. D **97**, 035001 (2018), arXiv:1708.09389 [hep-ph].
- [29] A. Ariga *et al.* (FASER), Phys. Rev. D **99**, 095011 (2019), arXiv:1811.12522 [hep-ph].
- [30] H. Abreu *et al.* (FASER), JINST **19**, P05066 (2024), arXiv:2207.11427 [physics.ins-det].
- [31] H. Abreu *et al.* (FASER), Phys. Lett. B **848**, 138378 (2024), arXiv:2308.05587 [hep-ex].
- [32] R. Mammen Abraham *et al.* (FASER), JHEP **01**, 199 (2025), arXiv:2410.10363 [hep-ex].
- [33] M. Bauer, O. Brandt, L. Lee, and C. Ohm, (2019), arXiv:1909.13022 [physics.ins-det].
- [34] O. Brandt *et al.* (ANUBIS), (2025), arXiv:2510.26932 [hep-ex].
- [35] V. V. Gligorov, S. Knapen, M. Papucci, and D. J. Robinson, Phys. Rev. D **97**, 015023 (2018), arXiv:1708.09395 [hep-ph].
- [36] G. Aielli *et al.*, Eur. Phys. J. C **80**, 1177 (2020), arXiv:1911.00481 [hep-ex].
- [37] S. Cerci *et al.*, JHEP **06**, 110 (2022), arXiv:2201.00019 [hep-ex].
- [38] O. Salin, A. Barr, J. McFayden, J. Boyd, M. Vranjes Milosavljevic, N. Vranjes, M. D’Onofrio, C. Gwilliam, J. K. Anders, S. Jakobsen, H. Otono, M. Queitsch-Maitland, B. J. Wilson, K. Lohwasser, M. V. Diwan, M. Vicenzi, and W. Wu, (2025).
- [39] J. L. Pinfold, Universe **5**, 47 (2019).
- [40] J. L. Pinfold, Phil. Trans. Roy. Soc. Lond. A **377**, 20190382 (2019).
- [41] J. P. Chou, D. Curtin, and H. J. Lubatti, Phys. Lett. B **767**, 29 (2017), arXiv:1606.06298 [hep-ph].
- [42] C. Alpigiani *et al.* (MATHUSLA), (2018), arXiv:1811.00927 [physics.ins-det].
- [43] C. Alpigiani *et al.* (MATHUSLA), (2020), arXiv:2009.01693 [physics.ins-det].
- [44] B. Aitken *et al.* (MATHUSLA), (2025),

- arXiv:2503.20893 [physics.ins-det].
- [45] CERN, “CERN Medium-Term Plan for the period 2026–2030: <https://cds.cern.ch/record/2941417/files/English.pdf>,” (2025).
- [46] R. Beltrán, C. Hati, M. Hirsch, and A. Martín-Galán, (2025), arXiv:2510.26946 [hep-ph].
- [47] S. Patrone, N. Blinov, and R. Plestid, (2025), arXiv:2509.14310 [hep-ph].
- [48] Y. Ema, P. J. Fox, M. Hostert, T. Menzo, M. Pospelov, A. Ray, and J. Zupan, (2025), arXiv:2507.15271 [hep-ph].
- [49] Z. S. Wang, Y. Zhang, and W. Liu, JHEP **01**, 070 (2025), arXiv:2409.18424 [hep-ph].
- [50] S. K. A, S. Das, A. Das, and S. Mandal, (2025), arXiv:2508.10734 [hep-ph].
- [51] A. Ahmed, Z. Chacko, N. Desai, S. Doshi, C. Kilic, S. Najjari, and R. P. R. Sudha, (2025), arXiv:2512.09046 [hep-ph].
- [52] R. E. Shrock, Phys. Lett. B **96**, 159 (1980).
- [53] R. E. Shrock, Phys. Rev. D **24**, 1232 (1981).
- [54] R. E. Shrock, Phys. Rev. D **24**, 1275 (1981).
- [55] A. M. Abdullahi *et al.*, J. Phys. G **50**, 020501 (2023), arXiv:2203.08039 [hep-ph].
- [56] R. N. Mohapatra and J. C. Pati, Phys. Rev. D **11**, 2558 (1975).
- [57] M. Bando and K. Yoshioka, Prog. Theor. Phys. **100**, 1239 (1998), arXiv:hep-ph/9806400.
- [58] C.-W. Chiang, G. Cottin, A. Das, and S. Mandal, JHEP **12**, 070 (2019), arXiv:1908.09838 [hep-ph].
- [59] I. Doršner, S. Fajfer, A. Greljo, J. F. Kamenik, and N. Košnik, Phys. Rept. **641**, 1 (2016), arXiv:1603.04993 [hep-ph].
- [60] F. Kling and S. Trojanowski, Phys. Rev. D **97**, 095016 (2018), arXiv:1801.08947 [hep-ph].
- [61] J. C. Helo, M. Hirsch, and Z. S. Wang, JHEP **07**, 056 (2018), arXiv:1803.02212 [hep-ph].
- [62] G. Aielli *et al.* (CODEX-b), Eur. Phys. J. C **80**, 1177 (2020), arXiv:1911.00481 [hep-ex].
- [63] A. Ariga *et al.* (FASER), (2019), arXiv:1901.04468 [hep-ex].
- [64] M. Hirsch and Z. S. Wang, Phys. Rev. D **101**, 055034 (2020), arXiv:2001.04750 [hep-ph].
- [65] J. De Vries, H. K. Dreiner, J. Y. Günther, Z. S. Wang, and G. Zhou, JHEP **03**, 148 (2021), arXiv:2010.07305 [hep-ph].
- [66] M. Ovchinnikov, V. Kryshnal, and K. Bondarenko, JHEP **02**, 056 (2023), arXiv:2209.14870 [hep-ph].
- [67] J. Y. Günther, J. de Vries, H. K. Dreiner, Z. S. Wang, and G. Zhou, JHEP **01**, 108 (2024), arXiv:2310.12392 [hep-ph].
- [68] D. Fargion, M. Y. Khlopov, R. V. Konoplich, and R. Mignani, Phys. Rev. D **54**, 4684 (1996).
- [69] D. Fargion, Y. A. Golubkov, M. Y. Khlopov, R. V. Konoplich, and R. Mignani, JETP Lett. **69**, 434 (1999), arXiv:astro-ph/9903086.
- [70] F. Domingo, J. Günther, J. S. Kim, and Z. S. Wang, Eur. Phys. J. C **84**, 642 (2024), arXiv:2308.07371 [hep-ph].
- [71] F. Domingo, J. Günther, J. S. Kim, and Z. S. Wang, “Displaced Decay Counter: <https://github.com/wzeren/Displaced-Decay-Counter>,” (2025).
- [72] A. Aguilar-Arevalo *et al.* (PIENU), Phys. Rev. D **97**, 072012 (2018), arXiv:1712.03275 [hep-ex].
- [73] D. A. Bryman and R. Shrock, Phys. Rev. D **100**, 073011 (2019), arXiv:1909.11198 [hep-ph].
- [74] F. Bergsma *et al.* (CHARM), Phys. Lett. B **166**, 473 (1986).
- [75] E. Cortina Gil *et al.* (NA62), Phys. Lett. B **807**, 135599 (2020), arXiv:2005.09575 [hep-ex].
- [76] B. Bloch-Devaux *et al.* (NA62), Phys. Lett. B **872**, 140119 (2026), arXiv:2507.07345 [hep-ex].
- [77] K. Abe *et al.* (T2K), Phys. Rev. D **100**, 052006 (2019), arXiv:1902.07598 [hep-ex].
- [78] R. Barouki, G. Marocco, and S. Sarkar, SciPost Phys. **13**, 118 (2022), arXiv:2208.00416 [hep-ph].
- [79] P. Abreu *et al.* (DELPHI), Z. Phys. C **74**, 57 (1997), [Erratum: Z.Phys.C 75, 580 (1997)].
- [80] G. Aad *et al.* (ATLAS), Phys. Rev. Lett. **131**, 061803 (2023), arXiv:2204.11988 [hep-ex].
- [81] A. Hayrapetyan *et al.* (CMS), Phys. Rev. D **110**, 012004 (2024), arXiv:2402.18658 [hep-ex].
- [82] M. Ovchinnikov, J.-L. Tastet, O. Mikulenko, and K. Bondarenko, Phys. Rev. D **108**, 075028 (2023), arXiv:2305.13383 [hep-ph].
- [83] K. Bondarenko, A. Boyarsky, D. Gorbunov, and O. Ruchayskiy, JHEP **11**, 032 (2018), arXiv:1805.08567 [hep-ph].
- [84] T. Sjöstrand, S. Ask, J. R. Christiansen, R. Corke, N. Desai, P. Ilten, S. Mrenna, S. Prestel, C. O. Rasmussen, and P. Z. Skands, Comput. Phys. Commun. **191**, 159 (2015), arXiv:1410.3012 [hep-ph].
- [85] L. Canetti and M. Shaposhnikov, JCAP **09**, 001 (2010), arXiv:1006.0133 [hep-ph].
- [86] N. Aghanim *et al.* (Planck), Astron. Astrophys. **641**, A6 (2020), [Erratum: Astron.Astrophys. 652, C4 (2021)], arXiv:1807.06209 [astro-ph.CO].